Available online at www.sciencedirect.com
SCIENCE DIRECT®
International Journal of Pharmaceutics 263 (2003) 133–140
international journal of pharmaceutics
www.elsevier.com/locate/ijpharm

Poly(butylcyanoacrylate) nanoparticles for topical delivery of 5-fluorouracil

M. Simeonova [a,*], R. Velichkova [a], G. Ivanova [b], V. Enchev [b], I. Abrahams [c]

[a] *Laboratory of Amphiphilic and Nonionogenic Polymers, Institute of Polymers, Bulgarian Academy of Sciences, Acad. G. Bonchev Str., bl. 103A, 1113 Sofia, Bulgaria*
[b] *Institute of Organic Chemistry, Bulgarian Academy of Sciences, Acad. G. Bonchev Str., bl. 9, 1113 Sofia, Bulgaria*
[c] *Structural Chemistry Group, Department of Chemistry, Queen Mary, University of London, Mile End Road, London E1 4NS, UK*

Received 7 May 2003; received in revised form 23 June 2003; accepted 25 June 2003

Abstract

Poly(butylcyanoacrylate) nanoparticles (PBCN) as a drug carrier of 5-fluorouracil (5FU) intended for topical treatment of skin lesia were investigated. The presence of 5FU (as saline solution, pH 10–11) in the polymerization medium affected the polymerization as well as the nanoparticle formation by influencing the initiation of the polymerization reaction. 5FU acted as an initiator in the anionic polymerization of *n*-butylcyanoacrylate monomer through its nucleophilic nitrogen centers. The results obtained by GPC, ^{1}H NMR, and X-ray diffraction allude to a possible mechanism of cytostatic immobilization in the polymer matrix, with evidence for both free and bound forms of the drug.

Keywords: Poly(butylcyanoacrylate) nanoparticles; 5-Fluorouracil; 5-Fluorouracil-loaded nanoparticles; Drug carriers; NMR; X-ray diffraction

1. Introduction

5-Fluorouracil (5FU; Fig. 1) is one of the most frequently used pyrimidine antimetabolites in the chemotherapy of cancer, including topical 5FU treatment of epidermal dysplasia. Its primary mechanism of action is thought to be inhibition of DNA synthesis by competitive inhibition of thymidylate synthetase, which is the target enzyme for 5FU (Goette, 1981; Bethesda, 1993). Indeed, Eaglestein et al. (1970) have estimated a tissue concentration of 5FU after intradermal injection that provides a minimal dose for thymidylate synthetase activity inhibition. Recently, McCarron et al. (1997) have confirmed that 5FU arrests the division of HeLa cells at the same range concentration. Topical 5FU is a cheap, convenient, and selective treatment of actinic keratoses (Goette and Odom, 1980; Pearlman, 1991). A general disadvantage for these formulations, containing a free drug solution is the short exposure of skin lesia to therapeutic drug concentrations due to low drug retention in the tumor tissue and the necessity of increased treatment frequency. Intralesional sustained-release chemotherapy with 5FU/epinephrine injectable gel provides an alternative non-surgical treatment for basal cell carcinomas (BCCs) (Yu et al., 1995; Miller et al., 1997). The main advantage of the 5FU gel formulation as a drug delivery system is that local therapeutic drug concentrations can be maintained longer than with a simple solution of the drug. These injectable gels used a biodegradable carrier matrix (bovine collagen), which can degrade on long-term storage.

* Corresponding author. Tel.: +359-2-979-22-85; fax: +359-2-870-75-23.
E-mail address: msimeon@polymer.bas.bg (M. Simeonova).

0378-5173/$ – see front matter © 2003 Elsevier B.V. All rights reserved.
doi:10.1016/S0378-5173(03)00373-9

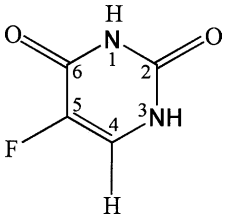

Fig. 1. 5-Fluorouracil (5FU).

Bioadhesive poly(butylcyanoacrylate) nanoparticles (PBCN) used as a sustained drug delivery system offers the possibility of improvement of the therapeutic index and frequency of topical 5FU treatment. Kreuter and Hartmann (1983) demonstrated an enhanced efficacy of 5FU against subcutaneously implanted Crocker sarcoma S 180 after i.p. injection of PBCN-bound 5FU. Unfortunately, this effect was accompanied by increased toxicity caused by prolonged accumulation of the drug in all organs examined. We believe that this undesirable side effect could be minimized or even avoided by local application of PBCN-bound 5FU.

The basic structure of 5FU is shown in Fig. 1. Ionization of 5FU occurs at high pH, with several possible anionic forms (Wierzchowski et al., 1965; Jang et al., 2001). Of interest is the possibility that nucleophilic centers in both molecular and anionic forms of 5FU could act as initiators for the polymerization of butylcyanoacrylate monomer. For this reason, an investigation of the influence of 5FU on the polymerization process was carried out.

The aim of the present study was to assess PBCN as a drug carrier of 5FU intended for topical treatment of skin lesia and to examine the nature of the interaction between butylcyanoacrylate monomer and the commercial form of the cytostatic during nanoparticle formation.

2. Materials and methods

2.1. Materials

n-Butylcyanoacrylate monomer was obtained from the Research Center for Special Polymers, Bulgaria. Dextran 40 was obtained from Pharmachim (Bulgaria) and citric acid from POCH (Poland). Commercially produced 5FU was used as delivered as a 0.5% (w/v) saline solution from Ebewe Arzneimittel GmbH (Pharmaceutical Laboratories, Austria). Other materials were of standard laboratory grade.

2.2. Preparation of unloaded PBCN

Unloaded PBCN were prepared by spontaneous anionic polymerization of butyl-2-cyanoacrylate monomer (20 mg/ml) in an aqueous medium containing 0.2% (w/v) citric acid and 0.8% (w/v) dextran 40. Polymerization was carried out under magnetic stirring and room temperature for 3 h.

2.3. Preparation of 5FU-loaded PBCN

The preparation of 5FU-loaded PBCN was carried out using modifications of the preparation of unloaded PBCN. In order to optimize the preparation of 5FU-loaded PBCN, two basic methods were investigated: inclusion of the cytostatic in the polymer matrix during the polymerization (during the formation of nanoparticles) and adsorption of the drug on the surface of previously prepared nanoparticles. The final concentration of PBCN in all preparations was 20 mg/ml.

2.3.1. Method 1

5FU-loaded PBCN were prepared using a starting polymer/cytostatic weight ratio of 1:2. Polymerization was carried out using the method described above for the unloaded polymer, with the appropriate amount of 5FU saline solution (ca. pH 10–11) added to the acidic polymerization medium (ca. pH 2.3) (a) before addition of the monomer and (b) 1 h after the start of the polymerization process.

2.3.2. Method 2

In this case, the appropriate amount of 5FU saline solution (pH 10–11) was added to the polymer system 3 h after the start of the polymerization of the butyl-2-cyanoacrylate monomer (see unloaded PBCN) and was adsorbed on the polymer nanoparticle surface (1 h, room temperature and slight stirring). The starting polymer/cytostatic weight ratio was 1:2.

Unloaded and 5FU-loaded (by Method 1) polymer nanoparticles were analyzed by NMR, GPC, and X-ray diffraction. Samples were analyzed after

dialysis, performed once against distilled water, using cellulose Visking membrane (Serva, USA) at room temperature for 24 h to remove agents dissolved in the polymerization medium. Finally, the polymer suspensions were lyophilized on a Lyovac GT2 lyophilizer (FINN-AQUA) for 24 h (−30 °C/+30 °C). Additionally, samples obtained by Method 1a were analyzed by NMR before dialysis to estimate the quantities adsorbed and included in the polymer matrix. The polymer samples from polymer suspension obtained by Method 2 were filtered using 0.1 μm pore sized membrane, washed with distilled water, and dried to powder in air to perform the above analyses.

2.4. Determination of particle size and loading capacity

The diameter of unloaded nanoparticles was determined by photon correlation spectroscopy (PCS), using a Malvern 4700 C nanosizer (Malvern Instruments, UK).

The degree of loading of 5FU in the polymer matrix was determined spectrophotometrically using a Perkin Elmer spectrophotometer, after filtration over a 0.1 μm pore sized membrane of portions of the polymer suspensions both obtained by Method 1a (prior dialysis) and Method 2. Drug concentration in the filtrate was determined by direct spectrophotometric analysis at 267 nm. Loading efficiency is given according to Labib et al. (1991):

$$\%\,\text{loading} = 100 \times \frac{\text{initial concentration} - \text{concentration in filtrate}}{\text{initial concentration}}$$

2.5. Gel permeation chromatography (GPC)

GPC was carried out using a Waters 150 GPC system with refractive index (Waters R401) and UV (Waters 486) detectors. The chromatograms were recorded with double simultaneous detection at a wavelength of 254 nm. Three *ultra*-Styragel columns with nominal pore sizes of 100 and 1000 Å, and linear were used. Tetrahydrofuran (THF) was used as the eluent, with a flow rate of 1 ml/min, at 45 °C. Samples were prepared as solutions in THF (14–16 mg dried nanoparticles were dissolved in 4 ml THF). After filtration through a 0.45 μm filter, 200 μl of every prepared solution was injected into chromatographic system. Elution volumes were referenced to toluene as an internal standard. Calibration was carried out with polystyrene standards.

2.6. Quantum-chemical calculations

The ab initio calculations were carried out using the GAMESS program package (Schmidt et al., 1993). The structure optimizations for 5FU and its anions were performed at the MP2/6-31+G** level without any constrains (C_1 symmetry). The mean gradient threshold was 0.0001 Hartree/Bohr.

2.7. ^1H NMR measurements

Unloaded and 5FU-loaded nanoparticles were prepared for NMR measurements as described above (see Section 2). Then, dried nanoparticles (10 mg) were dissolved in 0.6 ml deuterated-dimethyl sulfoxide (DMSO-d_6). The NMR spectra were obtained on a Bruker DRX-250 spectrometer operating at 250.13 MHz for ^1H, using a dual 5 mm probe head. The measurements were carried out at ambient temperature (ca. 300 K). All spectra were internally referenced to the signal of the solvent, set to 2.49 ppm. The one-dimensional (1D) and two-dimensional (2D) NMR spectra were obtained using the standard Bruker software: zg, cosy45, and cosydftp. The typical conditions for the 1D experiment were: 30° pulses, 1 s relaxation delays, 16 K time domain points, zero-filled to 32 K. Hard pulses with 90° pulse widths of 11.4 μs for ^1H at a power level of 3 dB below the maximum output were used. The 2D $^1H/^1H$ homonuclear correlation spectra (COSY) were performed with a spectral width of approximately 1000 Hz, relaxation delay 2 s, mixing pulse width 45°, number of increments 256 or 512, and FT size 1 K × 1 K.

2.8. X-ray powder diffraction

X-ray powder diffraction data were collected on an automated Philips PW 1050/30 diffractometer using Ni filtered Cu K radiation ($\lambda = 1.5418$ Å), in flat plate $\theta/2\theta$ geometry, over the 2θ range 5–70°, with a step width of 0.05° and a scan time of 2 s per step.

3. Results and discussion

The diameter of the unloaded polymer nanoparticles determined by PCS was 129 ± 29 nm. The amount of 5FU included in PBCN by adsorption (Method 2) and by Method 1a was 68.14 and 72.90%, respectively, of the total (initial) amount added.

The comparison of molecular weight profiles for unloaded PBCN and 5FU-loaded PBCN showed no increase in the molecular weight of the polymer, when the butyl-2-cyanoacrylate monomer was polymerized in the presence of 5FU as a saline solution (Method 1a). No changes in the shape of the GPC profile of 5FU-loaded polymer were observed. When PBCN were loaded by adsorption (Method 2), the addition of 5FU to the polymer suspension induced disappearance of the lower molecular weight fraction through a slight shift to higher molecular weight values as evidenced by changes in the GPC profile in comparison to unloaded nanoparticles (Fig. 2c). GPC measurements of 5FU-loaded polymer samples, using simultaneous double detection show an interaction/association between the polymer and 5FU (Fig. 2b and c), since the polymer peak detected via the refractive index had the same retention time as 5FU. The GPC chromatogram of 5FU alone indicates a higher retention time (lower molecular weight) for free 5FU than for 5FU-loaded nanoparticles (Fig. 2d).

^{1}H NMR spectra of the unloaded polymer, free 5FU as well as of the 5FU-loaded polymers produced by Methods 1 and 2 described above are presented in Fig. 3. The assignment of the spectra was achieved by analysis of ^{1}H NMR spectra and supported by the coupling patterns observed in the 2D ^{1}H/^{1}H correlated (COSY) NMR spectra. The ^{1}H NMR spectrum of the unloaded polymer shows broad resonance peaks at 0.88 ppm (CH_3, triplet), 1.39 ppm (CH_2, quintet), 1.62 ppm (CH_2, multiplet), 4.12 ppm (CH_2, triplet), and at 2.59 ppm (CH_2, multiplet), corresponding to the protons belonging to the *n*-butoxycarbonyl group and those of methylene protons from the polymer chain, respectively (Fig. 3a). ^{1}H NMR spectra of 5FU-loaded polymer samples produced by Method 1 in addition contain three sets of weak resonance peaks corresponding to three forms of 5FU present in the polymer matrix (Fig. 3). Three signals with different multiplicities and intensities were observed in the spectral region $\delta = 7.7$–8.1 ppm and assigned to H-4 of one free

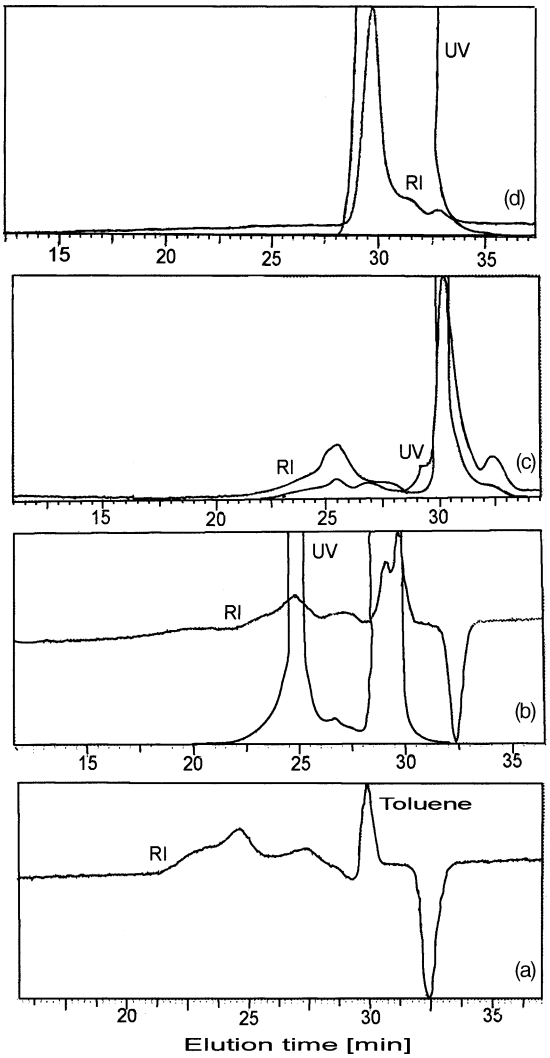

Fig. 2. Comparative GPC profiles obtained with double detection (refractive index and UV). (a) Unloaded PBCN; (b) 5FU-loaded nanoparticles by Method 1a; (c) 5FU-loaded nanoparticles by Method 2; and (d) 5FU free.

and two polymer chain-bound forms of 5FU. The resonance peak at 7.75 ppm in the spectrum of the sample produced by Method 1 appears as a triplet (overlapping doublet of doublets) and was assigned to H-4 of the free 5FU. The triplet arises due to spin–spin coupling H-4/H-3 ($^3J_{\text{H-4/H-3}} = 6.18$ Hz) and H-4/F-5 ($^3J_{\text{H-4/F-5}} = 6.15$ Hz). Two additional broad resonance peaks were observed in this region; a triplet at 7.96 ppm ($^3J_{\text{H-4/H-3}} = 5.87$ Hz, $^3J_{\text{H-4/F-5}} = 5.14$ Hz)

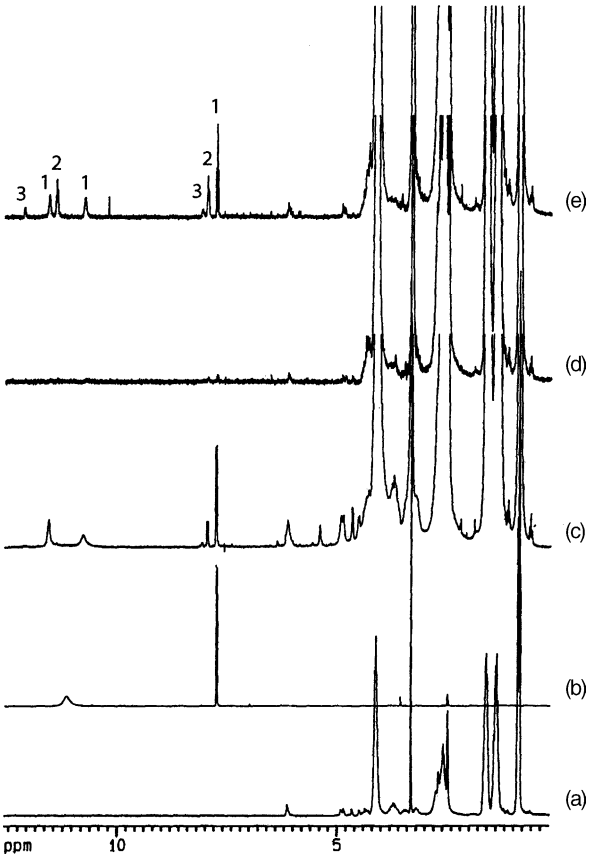

Fig. 3. ^{1}H NMR spectra. (a) Unloaded PBCN; (b) 5FU free; (c) 5FU-loaded nanoparticles by Method 2; (d) 5FU-loaded nanoparticles by Method 1b; (e) 5FU-loaded nanoparticles by Method 1a. Indication of the different (immobilized) forms of 5FU: ^{1}free (physically entrapped); ^{2}covalently immobilized at N-1 position; and ^{3}covalently immobilized at N-3 position.

and doublet at 8.07 ppm ($^{3}J_{\text{H-4/F-5}} = 6.11$ Hz), which were assigned to H-4 of 5FU covalently bonded to the polymer chain at N-1 and N-3, respectively. The resonance peaks at 10.71 and 11.51 ppm belong to H-3 and H-1 of free 5FU, while those at 11.34 and 12.06 ppm belong to H-3 and H-1 of 5FU substituted at N-1 and N-3, respectively. The multiplicity change and downfield shift of H-4 for two of the other forms of 5FU as well as the absence of resonance signals for H-1 or H-3 confirms the presence of 5FU covalently bonded to the polymer matrix and determines the position of the polymer constituent in the bound forms of 5FU. The ^{1}H NMR spectrum of 5FU-loaded polymer (Fig. 3c), obtained by Method 2, also contains three sets of signals corresponding to the different forms of 5FU discussed above. The peaks at 7.76 and 7.96 ppm belonging to H-4 of free and 5FU bonded to the polymer matrix at N-1 appear as doublets which are probably due to a fast intermolecular proton exchange of imino protons. Broad resonance peaks were observed at 10.75 and 11.52 ppm due to H-3 and H-1 of free 5FU and at 11.33 and 12.05 ppm due to H-3 and H-1 of 5FU substituted at N-1 and N-3, respectively. The assignment of the resonance peaks of 5FU agrees with the published data (Raic-Malic et al., 1999; Blicharska and Kupka, 2002; Xu et al., 2003).

On the basis of the integral intensities of the resonance peaks in the ^{1}H NMR spectra of 5FU-loaded PBCN produced by both methods, it was found that a visible amount of 5FU was included in the polymer matrix when 5FU was added to the polymerization medium before the monomer (Fig. 3e) and when nanoparticles were loaded by adsorption (Fig. 3c). The ratios of the three forms of 5FU (free:bonded at N-1:bonded at N-3) present in the samples produced by Methods 1a and 2 were found to be 1.00:1.16:0.16 and 1.00:0.30:0.01, respectively. The ratios of all forms of 5FU to the polymer were found to be 1.00:0.12 and 1.00:0.05 for Method 1a (prior dialysis) and Method 2, respectively. Samples from Method 1a, postdialysis, showed loss of approximately half the cytostatic with respect to the polymer. This indicates that at least 50% of 5FU is adsorbed with the remaining trapped in the polymer matrix.

X-ray powder diffraction data of 5FU-loaded polymers are shown in Fig. 4 and compared to the unloaded polymer (pattern b) and the calculated pattern of 5FU (pattern a) based on the known crystal structure (Fallon, 1973). The pattern for the 5FU-loaded polymer, loaded before the start of polymerization (pattern d), clearly shows crystalline Bragg peaks corresponding to crystalline 5FU. The presence of significant amounts of crystalline 5FU postdialysis suggests entrapment of microcrystals in the polymer matrix and is consistent with the observation of large polymer aggregates in this sample. In contrast, addition of 5FU 1 h after the initiation of polymerization yields a sample with no crystalline Bragg peaks (pattern c) and is consistent with the absence of resonance peaks of 5FU in this sample by ^{1}H NMR.

The main peculiarity of the open anionic polymerization of butyl-2-cyanoacrylate is that the

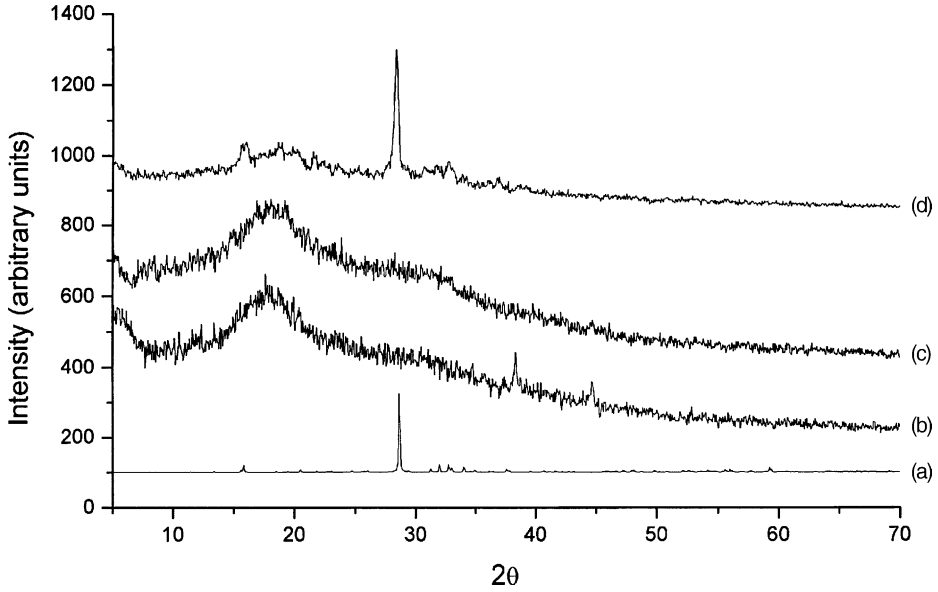

Fig. 4. X-ray powder diffraction patterns of: (a) free 5FU (calc.); (b) unloaded PBCN; (c) 5FU-loaded nanoparticles by Method 1b; (d) 5FU-loaded nanoparticles by Method 1a.

polymerization medium generates simultaneously both initiator (OH^-) and terminating agent (H^+), Scheme 1. Their relative concentrations dictate the degree of polymerization of the alkylcyanoacrylate monomers (Leonard et al., 1966; Ermosele et al., 1989) and hence the extent of nanoparticle formation (Lenaerts et al., 1989; Lescure et al., 1992). In the case of preparations in presence of 5FU as saline solution, added either before the monomer or shortly after in the polymerization medium, polymer aggregates were obtained with a low yield of nanoparticles. In fact, the pH increases because of the basic nature of the 5FU saline solution and enhances the polymerization kinetics. This led to a faster polymerization that did not allow for the formation of colloidal nanoparticles and as a result polymer aggregates were predominantly formed. In addition, pH is an important parameter in determining the stability of different molecular species of the pyrimidine bases (Wierzchowski et al., 1965). Depending on the pH of the medium, 5FU may exist in two anionic forms, A(N-1$^-$) and A(N-3$^-$), presented in Scheme 2. Quantum-chemical calculations performed at the MP2/6-31+G* level of theory in the gas phase predict that A(N-3$^-$) is more stable in energy by 12.53 kcal/mol, which is in agreement with the recently published data by Jang et al. (2001). However, these authors have shown that in aqueous solution A(N-1$^-$) is thermodynamically more stable by 2.44 kcal/mol. The calculated electron charges for 5FU and its possible anionic forms are listed in

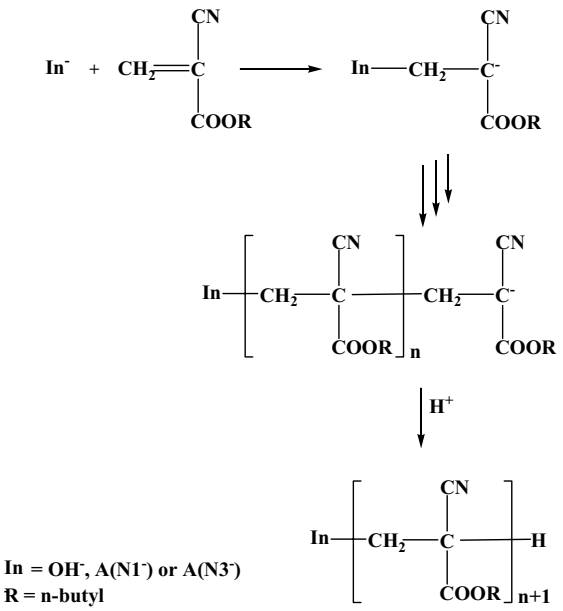

Scheme 1. Anionic polymerization of alkylcyanoacrylates.

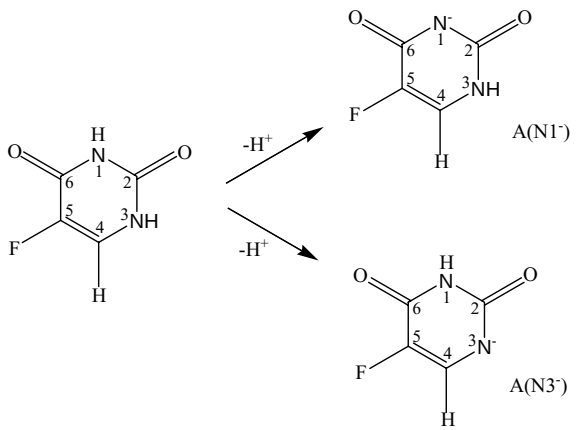

Scheme 2. pH-dependent ionization of 5FU.

Table 1. It was found that in the neutral molecule and both anions, electron density at the N-1 position is higher than that at N-3, which defines their nucleophilicity. The presence of 5FU in the polymerization medium could affect the polymerization as well as the nanoparticle formation through an influence on the initiation of the polymerization reaction. The initiation of anionic polymerization by 5FU (Scheme 1) could occur through the nucleophilic N-1 and N-3 centers. Bearing in mind this possibility, we performed investigations of the products obtained to verify the role of 5FU as an initiator of the polymerization of butyl-2-cyanoacrylate, as well as the mechanism of cytostatic immobilization in the polymer matrix.

The results discussed above allude to a possible mechanism of cytostatic immobilization in the polymer matrix. It is well known that *N*-alkylation of uracil and thymine can generally occur at N-3 of the pyrimidine ring, although a selective alkylation at the N-1 position is also known (Nagase et al., 1988; Gupta et al., 2000). The quantum-chemical calculations show that N-1 is the more electronegative center for 5FU and both possible anionic forms (Scheme 2). A(N-1$^-$) and A(N-3$^-$) are close in energy, despite this A(N-1$^-$) is thermodynamically more stable in water solution by 2.44 kcal/mol (Jang et al., 2001). The anionic polymerization of butyl-2-cyanoacrylate monomer in the presence of 5FU should be initiated predominantly by the more nucleophilic center, N-1 (see Scheme 2). ^{1}H NMR and GPC data corroborate the presence of 5FU covalently bound to the polymer chain in the cytostatic-loaded polymer produced by Method 1a. In addition, ^{1}H NMR and X-ray data are consistent with the presence of 5FU physically entrapped within the polymer matrix. The ^{1}H NMR data showed the presence of three forms of 5FU: free 5FU and two polymer-bound forms (at N-1 and at N-3). The X-ray data suggest that the amount of entrapped 5FU is significant, since they are able to form crystals of sufficient size to generate crystalline Bragg peaks in the powder diffraction pattern, corresponding to the known crystal structure of 5FU.

Table 1
Calculated total energies (in a.u.) and atomic charges (in e$^-$) for 5FU at MP2/6-31+G** level and its anionic forms A(N-1$^-$) and A(N-3$^-$) shown in Scheme 2

Atom	5FU	A(N-1$^-$)	A(N-3$^-$)
N-1	−0.743	−0.506	−0.609
N-3	−0.624	−0.496	−0.436
C-2	0.883	0.510	0.524
C-6	0.623	0.463	0.491
O-2	−0.626	−0.623	−0.619
O-6	−0.564	−0.556	−0.605
Total energy	−512.699896	−512.148086	−512.166443

Interestingly, the GPC chromatogram (Fig. 2c) and ^{1}H NMR spectrum (Fig. 3c) of PBCN loaded with 5FU by adsorption (Method 2) indicated interaction between the preformed polymer nanoparticles and the drug. A possible explanation is that at the low pH used, polymerization was incomplete when the basic 5FU saline solution was added. This observation is in agreement with an earlier report by Gaspar et al. (1991) on adsorption of primaquine on polyisohexylcyanoacrylate nanoparticles.

4. Conclusions

This work presents the approach to preparation of 5FU-loaded PBCN during the polymerization of *n*-butylcyanoacrylate monomer in presence of 5FU saline solution (pH = 10–11) as well as the loading of preformed nanoparticles by adsorption.

It was found that in the presence of basic 5FU solution in the polymerization medium, polymer aggregates were mainly obtained with a low yield of nanoparticles. This fact emphasizes the important role of the pH of the polymerization medium for formation of 5FU-loaded PBCN. Additionally, the high pH of

the medium determines the existence of two anionic forms of 5FU.

The investigation performed allowed to determine the role of 5FU as an initiator of the anionic polymerization of *n*-butylcyanoacrylate by its nucleophilic centers (N-1 and N-3). The results obtained strongly suggested that part of 5FU was covalently bound to the polymer chain at both N-1 (mainly) and N-3.

The polymer products obtained in the presence of 5FU during the polymerization were unfit for biological testing, since they consisted predominantly of polymer aggregates. However, the nanoparticle suspension loaded with 5FU saline solution through adsorption of the drug on previously prepared nanoparticles was considered suitable to perform further biological tests, which are in progress.

Acknowledgements

Financial support for this study from the Bulgarian Scientific Fund is gratefully acknowledged.

References

Bethesda, M.D., 1993. Fluorouracil. In: McEvoy, G.K. (Ed.), American Hospital Formulacy Service Drug Information. American Society of Hospital Pharmacists, pp. 573–577.

Blicharska, B., Kupka, T., 2002. Theoretical DFT and experimental NMR studies on uracil and 5-fluorouracil. J. Mol. Struct. 613, 153–166.

Eaglestein, W.H., Weinstein, G.D., Frost, P., 1970. Fluorouracil: mechanism of action in human skin and actinic keratosis. 1. Effect on DNA synthesis in vivo. Arch. Dermatol. 101, 132–139.

Ermosele, I.C., Pepper, D.C., Ryan, B., 1989. Water effect on the zwitterionic polymerisation of cyanoacrylates. Makromol. Chem. 190, 1613–1622.

Fallon III, L., 1973. The crystal and molecular structure of 5-fluorouracil. Acta Crystallogr. Sect. B 29, 2549–2556.

Gaspar, R., Preat, V., Roland, M., 1991. Nanoparticles of polyisohexylcyanoacrylate (PIHCA) as carriers for primaquine: formulation, physico-chemical characterization and acute toxicity. Int. J. Pharm. 68, 111–119.

Goette, D.K., 1981. Topical chemotherapy with 5-fluorouracil. J. Am. Acad. Dermatol. 4, 633–649.

Goette, D.K., Odom, R.B., 1980. Successful treatment of keratoacanthoma with intralesional 5-fluorouracil. J. Am. Acad. Dermatol. 2, 212–216.

Gupta, O.D., Twamley, B., Kirchmeier, R.L., Shreeve, J.M., 2000. Synthesis of *N*-polyfluorinated alkyl derivatives of uracil and 5-substitued uracils. X-ray structure of mono-*N*-substituted 5-trifluoromethyluracil. J. Fluorine Chem. 106, 199–204.

Jang, Y.H., Sowers, L.C., Cagin, T., Goddard III, W.A., 2001. First principles calculation of pK_a values for 5-substituted uracils. J. Phys. Chem. A 105, 274–280.

Kreuter, J., Hartmann, H.R., 1983. Comparative study on the cytostatic effects and the tissue distribution of 5-fluorouracil in a free form and bound to polybutylcyanoacrylate nanoparticles in sarcoma 180-bearing mice. Oncology 40, 363–366.

Labib, A., Lenaerts, V., Chouinard, F., Leroux, J.-Chr., Quellet, R., van Lier, J.E., 1991. Biodegradable nanospheres containing pthalocyanines and naphtalocyanines for targeted photodynamic tumor therapy. Pharm. Res. 8, 1027–1031.

Lenaerts, V., Raymond, P., Juhasz, J., Simard, M.A., Jolicoeur, C., 1989. New method for the preparation of cyanoacrylic nanoparticles with improved colloidal properties. J. Pharmacol. Sci. 78, 1051–1052.

Leonard, F., Kulkarni, R.K., Brandes, G., Nelson, J., Cameron, J., 1966. Synthesis and degradation of poly(alkyl α-cyanoacrylates). J. Appl. Polym. Sci. 10, 259–272.

Lescure, F., Zimmer, C., Roy, D., Couvreur, P., 1992. Optimization of polyalkylcyanoacrylate nanoparticle preparation: influence of sulfur dioxide and pH on nanoparticle characteristics. J. Colloid Interface Sci. 154, 77–86.

McCarron, P.A., Woolfson, A.D., McCafferty, D.F., Price, J.H., Sidhu, H., Hickey, G.I., 1997. Cytotoxicity of 5-fluorouracil released from a bioadhesive patch into uterine cervical tissue. Int. J. Pharm. 151, 69–74.

Miller, B.H., Shavin, J.S., Cognetta, A., Taylor, J.R., Salasche, S., Korey, A., Orenberg, E.K., 1997. Nonsurgical treatment of basal cell carcinomas with intralesional 5-fluorouracil/epinephrine injectable gel. J. Am. Acad. Dermatol. 36, 72–77.

Nagase, T., Seike, K., Shiraishi, K., Yamada, Y., Ozaki, S., 1988. Application of the benzyloxycarbonyloxymethyl moiety to a protective group of 5-fluorouracil. Selective alkylation of amide nitrogen of the uracil ring. Chem. Lett. 8, 1381–1384.

Pearlman, D.L., 1991. Weekly pulse dosing: effective and comfortable 5-fluorouracil treatment of multiple facial actinic keratoses. J. Am. Acad. Dermatol. 25, 665–667.

Raic-Malic, S., Hergold-Brundic, A., Nagl, A., Grdisa, M., Pavelic, K., 1999. Novel pyrimidine and purine derivatives of l-ascorbic acid: synthesis and biological evaluation. J. Med. Chem. 42, 2673–2678.

Schmidt, M.W., Baldridge, K.K., Boatz, J.A., Elbert, S.T., Gordon, M.S., Jensen, J.H., Koseki, S., Matsunaga, N., Ngugen, K.A., Su, S., Windus, T.L., Dupuis, M., Montgomery, J.A., 1993. General atomic and molecular electronic structure system. J. Comput. Chem. 14, 1347–1363.

Wierzchowski, K.L., Litonska, E., Shugar, D., 1965. Infrared and ultraviolet studies on the tautomeric equilibria in aqueous medium between monoanionic species of uracil, thymine, 5-fluorouracil, and other 2,4-diketopyrimidines. J. Am. Chem. Soc. 87, 4621–4629.

Xu, X., Yao, G., Li, Y., Lu, J., Lin, C., Wang, X., Kong, C., 2003. 5-Fluorouracil derivatives from the sponge *Phakellia fusca*. J. Nat. Prod. 66, 285–288.

Yu, N.Y., Orenberg, E.K., Luck, E.E., et al., 1995. Antitumor effect of intratumoral administration of fluorouracil/epinephrine injectable gel in C3H mice. Cancer Chemother. Pharmacol. 36, 27–34.